### Title

Purification of Lumbricus terrestris Mega-Hemoglobin for Diverse Oxygen Therapeutic Applications




### Journal

ACS Biomaterials Science & Engineering, 6(9)

### ISSN

2373-9878



### Authors

Savla, Chintan
Munoz, Carlos
Hickey, Richard
et al.



### Publication Date

2020-09-14

### DOI

10.1021/acsbiomaterials.0c01146

Peer reviewed

Published in final edited form as:

*ACS Biomater Sci Eng*. 2020 September 14; 6(9): 4957–4968. doi:10.1021/acsbiomaterials.0c01146.

# Purification of *Lumbricus terrestris* Mega-Hemoglobin for Diverse Oxygen Therapeutic Applications

**Chintan Savla**[1], **Carlos Munoz**[2], **Richard Hickey**[1], **Maria Belicak**[1], **Christopher Gilbert**[1], **Pedro Cabrales**[2], **Andre F. Palmer**[1,*]

[1]William G. Lowrie Department of Chemical and Biomolecular Engineering, The Ohio State University, Columbus, Ohio, USA

[2]Department of Bioengineering, University of California, San Diego, La Jolla, California, USA

## Abstract

Oxygen therapeutics are being developed for a variety of applications in transfusion medicine. In order to reduce the side-effects (vasoconstriction, systemic hypertension, and oxidative tissue injury) associated with previous generations of oxygen therapeutics, new strategies are focused on increasing the molecular diameter of hemoglobin obtained from mammalian sources via polymerization and encapsulation. Another approach towards oxygen therapeutic design has centered on using naturally occurring large molecular diameter hemoglobins (i.e. erythrocruorins) derived from annelid sources. Therefore, the goal of this study was to purify erythrocruorin from the terrestrial worm *Lumbricus terrestris* for diverse oxygen therapeutic applications. Tangential flow filtration (TFF) was used as a scalable protein purification platform to obtain a >99% pure LtEc product, which was confirmed by size exclusion high performance liquid chromatography and SDS-PAGE analysis. *In vitro* characterization concluded that the ultra-pure LtEc product had oxygen equilibrium properties similar to human red blood cells, and a lower rate of auto-oxidation compared to human hemoglobin, both of which should enable efficient oxygen transport under physiological conditions. *In vivo* evaluation concluded that the ultra-pure product had positive effects on the microcirculation sustaining functional capillary density compared to a less pure product (~86% purity). In summary, we purified an LtEc product with favorable biophysical properties that performed well in an animal model using a reliable and scalable purification platform to eliminate undesirable proteins.

## Graphical Abstract

[*]**Correspondence:** Andre F. Palmer, William G. Lowrie Department of Chemical and Biomolecular Engineering, The Ohio State University, 452 CBEC, 151 West Woodruff Avenue, OH 43210, USA. palmer.351@osu.edu. *Phone*: (614) 292-6033.

Conflicts of Interest

There are no conflicts to declare.

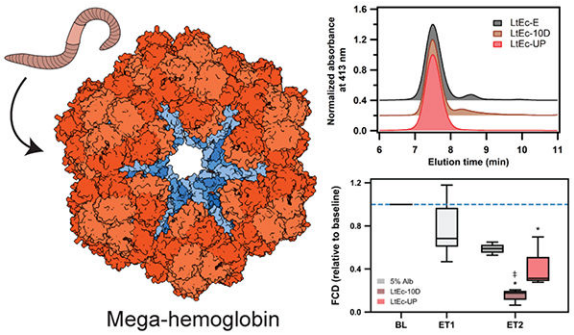


**Keywords**

megahemoglobin; erythrocruorin; hemoglobin-based oxygen carrier; oxygen therapeutic; tangential flow filtration; microcirculation

## 1. Introduction

Erythrocruorins (Ecs) are a class of hemoglobin (Hb) derived from annelids. Annelids do not have red blood cells (RBCs). Therefore, Ecs exist acellularly in annelids, and possess megastructures with molecular mass of ~3.6 MDa and diameter of ~30 nm[1–3]. Human Hb (hHb), for reference, has a molecular mass of 64.5 kDa and diameter of ~5.5 nm. Due to their small size, cell free Hb and Hb αβ dimers can extravasate through the blood vessel wall into the tissue space, where they can scavenge the vaso-regulatory molecule nitric oxide (NO), and elicit vasoconstriction, systemic hypertension and oxidative tissue injury[4]. The larger molecular diameter of Ec is expected to prevent extravasation through the blood vessel wall, and the associated side-effects associated with Hb infusion. *In vivo* biocompatibility studies have confirmed the reduced vasoactivity of Ec, and support the use of Ec in transfusion applications as a RBC substitute[5,6]. Other strategies to design RBC substitutes from the Hb precursor such as intra-molecularly cross-linked Hb[7], polymer surface conjugated (PEGylated) Hb[8–11], polymerized Hb[12], vesicle and liposome encapsulated Hb (LEHs)[13] and Hb submicron particles[14,15] focus on increasing the size of the Hb molecule in order to reduce extravasation, which in turn reduces vasoactivity and oxidative tissue injury. Due to the larger size of Ec (~ 30 nm) compared to mammalian Hbs (~5 nm), there is no need to further increase Ec size for transfusion applications.

This study focuses on Ec derived from the terrestrial worm *Lumbricus terrestris* (Lt), which is abundant in the United States. Apart from its large size, Ec derived from Lt is also known to be stable under physiological conditions and exhibits moderate affinity for oxygen[16]. However, Ecs derived from other annelids such as *Arenicola marina* (AmEc) possess extremely high oxygen affinity[17], whereas Ec from *Nereis virens* (NvEc) has high oxygen affinity and low cooperativity[18]. All of these equilibrium oxygen binding properties are important in order to assess the ability of Ecs to transport oxygen *in vivo*. The oxygen affinity of LtEc is moderate (28 mm Hg) which is comparable to that of human RBCs (26 mm Hg)[19]. Also, the higher cooperativity of LtEc as compared to hHb and other Ecs helps it bind and offload oxygen more effectively *in vivo*[16]. The kinetics of conversion of Hb from

the reduced form ($HbFe^{2+}$) to the oxidized form ($HbFe^{3+}$, methemoglobin [metHb] under physiological conditions is captured by the auto-oxidation rate constant. Human Hb oxidizes under physiological conditions with a rate constant of 0.043 $h^{-1}$ [12], whereas Ecs are known to oxidize ~10 × slower under the same conditions with an average rate constant of 0.004 $h^{-1}$ [16]. This unique property of Ecs allows them to retain their oxygen binding ability for longer duration in *in vivo* or *in vitro* systems compared to mammalian Hbs.

Therefore, the large size, moderate oxygen affinity, and low rate of auto-oxidation have opened up diverse applications for LtEc as an oxygen therapeutic. While the Ecs of some annelids such as *Glossoscolex paulistus* (Gp) are still in development and have been tested in animals in a limited capacity[20–22], LtEc, AmEc, and NvEc have found extensive biomedical applications. Hemarina™, a biopharmaceutical company based in France, has shown the potential of AmEc and NvEc in various animal models. In models of hypervolemic infusion (i.e. top load) and extreme anemia in golden Syrian hamsters, LtEc did not elicit vasoconstriction or hypertension and improved tissue oxygenation[6,23]. Similarly, AmEc had negligible effects on mean arterial pressure, heart rate, and microcirculatory vasoconstriction in an *in vivo* top load model[24,25]. Apart from the traditional use of oxygen therapeutics as a RBC substitute, NvEc has been used to enhance oxygen transport in a recombinant cell culture of CHO-S cells[26] and human mesenchymal stem cell cultures[18]. NvEc has also been used in an *in vitro* model for islet oxygenation, where it was found to be better than traditional perfluorocarbon-based oxygen carriers at restoring insulin secretion in a bio-artificial pancreas[27]. Furthermore, AmEc has been effective in facilitating cold static preservation of rat hearts before transplantation[28], preservation of porcine lungs to prevent ischemia reperfusion injury before transplantation in pigs[29], and dynamic preservation of porcine kidneys to prevent injury before transplantation in a pig model[30]. Because of the wide range of applications of Ecs, it is necessary to develop scalable purification methods to improve Ec purity.

Tangential flow filtration (TFF) based protein separation was determined to be more efficient and scalable as compared to other methods devised to extract and purify LtEc from worms such as ultracentrifugation[31] and metal salt precipitation[32]. However, due to a lack of quantitative assessment of impurities in the product, previously published protocols on LtEc purification using TFF have failed to achieve an ultrapure product[6,33]. Since LtEc is derived from a non-mammalian source, we decided that it was essential that the purification process yielded a product with minimal protein impurities in order to eliminate the possibility of eliciting side-effects *in vivo*. The Lt homogenate contains clotting proteins ~40 kDa in size, which could result in coagulation of the purified LtEc product if not separated[34]. Hence, quantitative assessment of impurity levels during the TFF process was necessary to ensure the highest purity product to enable a wide range of potential applications. The TFF process separates proteins using size as the dimension of heterogeneity. Standard protein purification techniques used to purify recombinant proteins from cell cultures utilize multiple chromatographic separation steps along with a size-based separation step to isolate target proteins. However, a recent study aimed at purifying LtEc using anion exchange and immobilized metal affinity chromatography showed that LtEc experienced high methemoglobin formation and dissociation into dodecameric subunits when purified using the two methods[35]. Furthermore, the study also observed that the product purified using

chromatographic techniques was less pure as compared to the product purified using TFF. Hence, the focus of this study was to purify LtEc using TFF to maximize product purity, characterize its biophysical properties, and test the material in an animal model to assess its biocompatibility. Quantitative assessment of impurity levels was performed by constant analysis of samples throughout the TFF process via size exclusion chromatography and gel electrophoresis. Both are well-known and reliable techniques to assess product purity. Further biophysical characterization was also performed to determine the biophysical properties of the purified LtEc; as well as, *in vivo* studies to determine the biocompatibility of the material and its ability to prevent the aforementioned side-effects.

## 2. Experimental section

### 2.1. Hb Purification

Human Hb (hHb) was purified via TFF as described previously in the literature[36].

### 2.2. LtEc Purification

LtEc was purified by modifying previously published LtEc purification protocols[6,16,33]. 1,000 Canadian Nightcrawlers (*Lumbricus terrestris)* were purchased from Wholesale Bait Company (Hamilton, OH) and stored at 4°C. Batches of worms were washed thoroughly in tap water to remove dirt and mucus, which were then blended in tris-EDTA buffer (10 mM tris-HCl, 1 mM EDTA, pH 7.0) until a smooth puree was obtained. The homogenate was centrifuged at 3,700 × g for 40 mins to pellet out the majority of worm debris and yielded a red supernatant. The resultant supernatant was centrifuged at 18,000 × g for 40 mins to further separate lighter debris and obtain a cloudy red supernatant for further processing. Throughout the centrifugation process, the temperature was maintained at 4 °C to limit LtEc oxidation. The cloudy red supernatant was then vacuum filtered over filter paper with particle retention of 4–8μm to restrict particulates from entering the subsequent TFF processing stage.

Figure 1 describes the TFF purification protocol. The pre-clarified LtEc solution was initially passed through a 0.65μm TFF cartridge (surface area = 1000 $cm^2$, polyether sulfone, Repligen, Waltham, MA) until a majority of the solution was collected on the permeate side. The filtrate from the 0.65μm TFF cartridge was then passed through a 0.22μm TFF cartridge (surface area = 1000 $cm^2$, polyether sulfone). Throughout this process, a transmembrane pressure of 7–8 psig was maintained to enable transmission of protein through the TFF cartridge. During the two initial TFF stages, there was substantial clogging of the filter membranes caused by the presence of protein aggregates, which was reduced by flushing deionized water through the permeate side of the filter to unclog the membrane surface pores. The 0.22 μm permeate was then subjected to constant volume diafiltration over a 500 kDa TFF cartridge (surface area = 750 $cm^2$, polysulfone) using a modified lactated Ringer's solution (115 mM NaCl, 4 mM KCl, 1.4 mM $CaCl_2.2H_2O$, 13 mM NaOH, 12.3 mM N-acetyl-L-cystine, 27 mM sodium lactate, pH 7.4). Permeate and retentate samples were collected after every diacycle and assessed via size exclusion high performance liquid chromatography coupled with size exclusion chromatography (SEC-HPLC) to monitor removal of smaller molecular weight (MW) species. Diafiltration was continued until the

purity of LtEc reached ~99% as assessed using SEC-HPLC, and <1% of smaller impurities were left in solution. The resulting pure protein solution was then concentrated on a 500 kDa filter to a concentration of ~100 mg/mL, sterilized by passing it through a 0.22 μm syringe filter, and stored at −80 °C until further use. TFF filters were sanitized using 0.5 M NaOH and stored in 0.1 M NaOH.

### 2.3. UV-Visible Spectrophotometry

Spectrophotometric absorbance measurements were obtained using a HP 8452A diode array spectrophotometer (Olis, Bogart, GA). Total Hb and metHb (i.e. oxidized Hb in the $Fe^{3+}$ valence state) concentrations were determined using the cyanmethemoglobin method[37] and verified by the Winterbourn equations[38] for hHb and methods described by Fanelli *et al.*[39,40] for LtEc. DeoxyHb samples were prepared by bubbling samples with $N_2$ followed by sodium dithionite ($Na_2S_2O_4$) addition. MetHb samples were prepared by oxidizing samples using potassium ferricyanide ($K_3Fe(CN)_6$).

### 2.4. SEC-HPLC

Samples were separated on an analytical Acclaim SEC-1000 (4.6 × 300 mm) column (Thermo Fisher Scientific, Waltham, MA) attached to a Dionex UltiMate 3000 UHPLC/HPLC system (Thermo Fisher Scientific, Waltham, MA). The mobile phase consisted of 50 mM sodium phosphate buffer (PB) at pH 7.4. Chromeleon 7 software was used to control and measure HPLC parameters such as flow rate (0.35 mL/min) and UV-visible absorbance detection (280 nm and 413 nm). All samples were filtered through 0.2 μm syringe filters before SEC-HPLC analysis. Elution peaks were identified and their respective areas under the curve (composition) were calculated. Purity was calculated by dividing the area of the LtEc peak by the total area of all the proteins peaks.

### 2.5. SDS-PAGE

Protein samples were diluted to ~1 mg/mL in deionized water and mixed with tris-glycine SDS sample buffer (Fisher Scientific, Pittsburgh, PA). Gradient 10–20% tris-glycine gels were loaded with 10 μg of sample per well and run at 225 V for 40 mins. Gels were stained with 1× Coomassie blue (Bio-Rad Laboratories) and destained (60% deionized water, 30% methanol, 10% acetic acid) overnight. Gel images were obtained using an image scanner. Densitometric analysis of the gel images was performed using ImageJ (National Institutes of Health, Bethesda, MD) software[41].

### 2.6. Oxygen Equilibrium Curves

$O_2$ equilibrium curves were obtained using a Hemox Analyzer (TCS Scientific Corp., New Hope, PA) using methods described previously in the literature[6]. Protein samples were diluted to ~60 μM (heme basis) in 5 mL Hemox buffer (pH 7.4) with 20 μL of Additive A, 20 μL of Additive B, and 20 μL of antifoaming solution (TCS Scientific). The temperature was maintained at 37.0 ± 0.1 °C. The Hill equation[42] was used to fit the data, and $P_{50}$ and n values were regressed from the curve fits.

### 2.7. Hydrodynamic Diameter

The hydrodynamic diameter of LtEc and hHb was measured using a BI-200SM goniometer (Brookhaven Instruments Corp., Holtsville, NY) at an angle of 90° and wavelength of 637 nm. Protein samples were diluted to ~0.5–1 mg/mL concentration in deionized water. The hydrodynamic diameter was obtained by using average values from the non-linear least squared (NNLS) algorithm in the instrument software.

### 2.8. Auto-Oxidation

LtEc and hHb samples were diluted to 60 μM (heme basis) in 50 mM PB (pH 7.4). A UV-visible spectrophotometer with an attached recirculating water bath was used to record absorbance measurements from 300–700 nm at 37° C every 30 mins for 10 hours. The auto-oxidation rate constant was determined by fitting first order kinetics to the disappearance of oxy-Hb/LtEc species in solution.

### 2.9. Rapid Deoxygenation Kinetics

Rapid kinetic measurements were obtained using methods described previously in the literature[43,44]. Protein samples were diluted to 12.5 μM (heme basis) in PBS (0.1 M, pH 7.4). Deoxygenated buffer was prepared by adding 1.5 mg/mL of sodium dithionite to PBS bubbled with $N_2$ for 20–30 mins. Deoxygenated buffer and oxygenated protein samples were mixed rapidly in a microvolume stopped-flow spectrophotometer (Applied Photophysics Ltd., Surrey, United Kingdom) and the absorbance was monitored at 437.5 nm. An exponential decay function was fit to the data and the rate constant for oxygen dissociation ($k_{off,O_2}$) was determined for each sample.

### 2.10. Viscosity and Colloid Osmotic Pressure

Viscosity was measured at a shear rate of 160/sec (Brookfield Engineering Laboratories, Middleboro, MA). Colloid osmotic pressure (COP) was measured using a 4420 Colloid Osmometer (Wescor, Logan, UT).

### 2.11. Window Chamber Animal Preparation

Animal handling and care followed the NIH guide for the care and use of laboratory animals and the experimental protocol was approved by the local animal care committee at the University of California, San Diego. Studies were performed in 55 to 65 g male Golden Syrian hamsters (Charles River Laboratories, Boston, MA) fitted with a dorsal skinfold window chamber. The hamster window chamber model is widely used for microvascular studies without anesthesia. The complete surgical technique was described previously in the literature[45]. Arterial and venous catheters filled with heparinized saline solution (30 IU/mL) were implanted into the carotid and jugular vessels. Catheters were tunneled under the skin, exteriorized at the dorsal side of the neck, and securely attached to the window frame.

### 2.12. Inclusion Criteria

Animals were considered suitable for experiments if systemic parameters were as follows: heart rate (HR) > 340 beats/min, mean arterial blood pressure (MAP) > 80 mm Hg, systemic hematocrit (Hct) > 45%, and arterial $O_2$ partial pressure ($pAO_2$) > 50 mm Hg. Additionally,

animals with signs of low perfusion, inflammation, edema, or bleeding in their microvasculature were excluded from the study.

### 2.13. Instrument Setup

The unanesthetized animal was placed in a restraining tube with a longitudinal slit from which the window chamber protruded, then fixed to the microscopic stage for transillumination with the intravital microscope (BX51WI, Olympus, New Hyde Park, NY). Animals were given 20 minutes to adjust to the tube environment and images were obtained using a CCD camera (4815, COHU, San Diego, CA). Measurements were carried out using a 40× water immersion objective (LUMPFL-WIR, numerical aperture 0.8, Olympus).

### 2.14. Systemic Parameters

Mean arterial pressure (MAP) and heart rate (HR) were monitored continuously (MP150, Biopac System Inc., Santa Barbara, CA). Hct was measured from centrifuged arterial blood samples taken in heparinized capillary tubes. Hb content was determined spectrophotometrically (B-Hemoglobin, Hemocue, Stockholm, Sweden). Arterial blood was collected in heparinized glass capillaries (50μL) and immediately analyzed for $pO_2$, $pCO_2$, and pH (ABL90; Radiometer America, Brea, CA). Arterial Hb saturations were measured using an IL482 CO-Oximeter (Instrumentation Laboratory, Lexington, MA).

### 2.15. Microhemodynamics

Arteriolar and venular blood flow velocities were measured using the photodiode cross-correlation method (Photo-Diode/Velocity, Vista Electronics, San Diego, CA)[46]. The measured centerline velocity (V) was corrected according to blood vessel size to obtain the mean RBC velocity[47]. A video image-shearing method was used to measure blood vessel diameter (D)[48]. Blood flow (Q) was calculated from the measured values using Equation 1.

$$Q = \pi \times V\left(\frac{D}{2}\right)^2 \quad \text{\#(Equation 1)}$$

### 2.16. Functional Capillary Density (FCD)

Functional capillaries, defined as capillary segments that have RBC transit of at least one RBC in a 60 second period in 10 successive microscopic fields, were assessed in a region measuring 0.46 $mm^2$. FCD ($cm^{-1}$) is calculated as the total length of RBC perfused capillaries divided by the area (0.46 $mm^2$).

### 2.17. Vascular Responses to LtEc

A 40% blood exchange transfusion (ET1) using 5% human serum albumin (HSA) was implemented on the animals before they were randomly exchanged transfused for an additional 20% of their blood volume (ET2) with 5% HSA, LtEc-10D (5 g/dL), or LtEc-UP (5 g/dL). Systemic and micro circulatory vascular responses were then studied 30 minutes before and after each exchange transfusion.

### 2.18. Statistical Analysis

Data within each group were analyzed using two-way analysis of variance for repeated measurements. When appropriate, post hoc analyses were performed with the Dunnett's multiple comparisons test. Microhemodynamic data are presented as ratios relative to baseline values and absolute values are reported in the figure legends. A ratio of 1.0 signifies no change from baseline, while lower and higher ratios are indicative of changes proportionally lower and higher than baseline (e.g., 1.5 represents a 50% increase from the baseline level). The same blood vessels and capillary fields were monitored throughout the study, such that direct comparisons to their baseline levels could be performed, allowing for more reliable statistics on small sample populations. All statistics were calculated using Prism 6 (GraphPad Software Inc., San Diego, CA). Changes were considered significant if p values were less than 0.05.

## 3. Results and Discussion

### 3.1. Purity of LtEc

We observed 7–8 distinct peaks corresponding to smaller MW proteins in permeate chromatograms (Figure 2A). As more diafiltrations were performed, the presence of smaller MW proteins decreased indicating successful removal of these species from the retentate. The peaks of smaller MW proteins in the retentate corresponded with those observed in the permeate chromatogram (Figure 2B). As the number of diafiltrations increased, we observed a reduction in the peak area of smaller MW proteins that were present in the LtEc homogenate indicating their removal from the retentate. The LtEc peak remained at the same intensity during diafiltration, since we had negligible LtEc transmission through the 500 kDa filter. The relative area under the curve of the LtEc peak is an indicator of the purity of the target protein in the final solution. We observed that the percentage purity of LtEc before diafiltration was ~43%, with the remainder corresponding to unwanted proteins. As the number of diafiltration cycles increased, LtEc purity reached 99.1% (Figure 2C). We determined that at least 28–30 diacycles were required to yield LtEc that was >99% pure. There was a small amount of batch-to-batch variability in the composition of the initial 500 kDa retentate, but it was determined that ~30 diafiltrations yielded a product with >99% purity. In previously published work on LtEc purification[6,49], the TFF purification process was stopped after 10 diafiltration cycles. Figure 2D compares SEC-HPLC chromatograms monitored at an absorbance of 413 nm for LtEc-E (a product previously purified in our lab[6]), LtEc-10D (a product recently replicated with the same processing conditions as LtEc-E), and LtEc-UP (a product purified using the improved purification method as discussed in this work). As observed, there was a trailing leg (elution time ~ 8.5 mins) in the SEC-HPLC chromatograms for LtEc-E and LtEc-10D indicating the presence of smaller MW components in substantial quantities. Both of these products (LtEc-E and LtEc-10D) were obtained after 10 diafiltrations. The LtEc purity achieved after 10 diacycles was ~86% with the presence of >10% unwanted proteins. The SEC-HPLC chromatogram for LtEc-UP showed no such trailing leg indicating a purer product compared to LtEc-E and LtEc-10D. Purification systems for recovery of recombinant therapeutic proteins derived from cell cultures utilize multiple chromatographic steps to achieve ultrapure products with impurities ranging from 10–100 ppm. However, the desired purity level of LtEc depends on the

intended biomedical application and if the presence of small amounts of impurities have the possibility of eliciting side-effects *in vivo*. Hence, assessment of LtEc biophysical properties and *in vivo* evaluation in a hamster window chamber model were used to test the biocompatibility of the materials (LtEc-10D and LtEc-UP). A recent study purified LtEc from earthworm homogenate using anion exchange (AEX) and immobilized metal affinity (IMAC) chromatography[35]. The results from that study suggested that both AEX and IMAC led to subunit dissociation of the LtEc megastructure and resulted in high levels of methemoglobin, thus affecting the quality of the purified LtEc. Furthermore, both purification techniques were unable to reduce endotoxin levels below 6 EU/mM heme. Hence, TFF based size separation of LtEc from worms presents a platform for scalable and efficient purification that produces a pure product without affecting the quality of the product.

Retentate samples were obtained from Stages 0, 1 and 2 and compared to LtEc-E, LtEc-10D and LtEc-UP using SDS-PAGE analysis (Figures 2E). We expected Stage 0 and 1 to have a wide variety of proteins present, since the MWCO of the membranes were large (0.65 and 0.22 μm). Lanes 1–3 showed a variety of protein bands ranging from 8 kDa to 72 kDa denoting the various components in the earthworm homogenate. Lanes 2 and 3 showed sequential reduction or disappearance of some bands indicating removal at each stage of the purification process. The band at ~55 kDa corresponded to the LtEc trimer (made up of globin chains), the band at ~13 kDa corresponded to one of the LtEc monomers (i.e. globin chains), and bands in the range 27–32 kDa corresponded to the linker proteins that hold the LtEc megastructure together[2,50]. There was a noticeable decrease in the trimer band (55 kDa) from S1 to S2, which denoted the retention of LtEc on the 0.22 μm filter. This may be due to the presence of aggregates and complexes that the LtEc protein may have formed with the clotting proteins in the coelomic fluid of the worm during the homogenization process[34]. The 0.22 μm filtration step was essential to eliminate bacteria in subsequent fractions. The fractions obtained after TFF purification were purer and contained fewer protein bands as observed in lanes 5–7. All three final product lanes contained a major trimer band, monomer band, and linker bands. The LtEc-UP lane had a very small amount of impurities in the 30–35 kDa region, which agreed with results from SEC-HPLC. The linker proteins that hold the LtEc mega-structure together are in the MW range ~28–36 kDa. According to a previous study, the MW of linker proteins were determined to be 24, 27, and 34 kDa[51]. Hence, a majority of the faint bands in the SDS-PAGE of our LtEc-UP product are also most likely the linker proteins. However, there may be a small amount of impurities in the same region contributing to the overall impurity of the product. On closer examination, it was observed that LtEc-E has two faint bands around ~15–17 kDa and darker bands in the 30–35 kDa region corresponding to the presence of unwanted proteins that were not eliminated in the purification process. Densitometric analysis concluded that these bands contributed to ~12% of the total protein. LtEc-10D also had extra bands at ~38 kDa which accounted for ~9.3% of the total protein in the lane, possibly due to dimer-like structures of the impurities observed in LtEc-E. Densitometric analysis also concluded that the faint bands in LtEc-UP were of lower intensity and accounted for ~1.4% of the total protein and hence were lower than LtEc-10D and LtEc-E, thus confirming lower levels of impurities and hence a higher purity product. Therefore, purity determination via SDS-

PAGE analysis further supported the SEC-HPLC results, and confirmed that LtEc-UP was a much purer product than both LtEc-10D and LtEc-E.

### 3.2. Process Improvements

After completing the initial centrifugation and vacuum filtration steps in the LtEc purification protocol, a cloudy supernatant was obtained which became slightly clear after passing it through a 0.65 μm TFF cartridge. Subsequent filtration through a 0.22 μm TFF cartridge yielded a clear red solution. However, during the course of processing, the 0.22 μm filter fouled multiple times and had to be flushed with DI water repeatedly while applying 7–8 psig of transmembrane pressure. Introduction of the 0.65 μm pre-filter reduced 0.22 μm filter fouling substantially, which in turn prolonged the lifetime of the 0.22 μm filter. The 500 kDa filtrate was predominantly yellowish-brown in color, whereas the retentate was bright red indicating the presence of LtEc protein in the retentate. A vacuum was maintained inside the retentate bottle of the 500 kDa system to effectively pull buffer and maintain continuous volume diafiltration. The 500 kDa filtrate became lighter in color as more diafiltration cycles were carried out indicating the gradual removal of smaller MW proteins.

### 3.3. Hydrodynamic Diameter

The size of the purified native protein is important in order to predict its' *in vivo* fate upon transfusion into the systemic circulation, such as extravasation through the blood vessel wall. Hb, due to its small size, extravasates through blood vessel walls, scavenging nitric oxide and eliciting vasoconstriction and hypertension[4]. Previous studies have determined the diameter of LtEc to be ~30 nm with a molecular mass of 3.5–3.6 MDa[1–3]. Our dynamic light scattering (DLS) results showed that the hydrodynamic diameter of LtEc-UP was 28 nm, while hHb was 6.5 nm (Figure 2F–H). The effective diameter of LtEc-10D was found to be ~24 nm which was lower than LtEc-UP but not significantly different as determined using a two-sample t-test. These results are also summarized in Table 1. This decrease may be explained by the contribution of smaller MW proteins in reducing the effective diameter down by a small value. Regardless, due to its larger size compared to hHb, LtEc is expected to remain in the lumen of blood vessels and should not extravasate into the tissue space. Previously, the LtEc diameter was reported to be ~80–90 nm[52,53] which was attributed to the possible presence of larger LtEc structures in aqueous solution. We did not observe such aggregation or dimerization in our samples. The presence of even a small amount of larger diameter particles (dust) is known to skew the overall effective diameter of particles in solution measured using DLS[54]. Hence, care was taken to keep our samples dust-free for DLS analysis in order to obtain accurate hydrodynamic diameter measurements.

### 3.4. Oxygen Binding and Offloading Characteristics

Oxygen equilibrium curves (OECs) enable assessment of the ability of Hb-based oxygen carriers (HBOCs) to bind and offload oxygen. The OECs were fit to the Hill equation to regress the $P_{50}$ (oxygen affinity) and n (cooperativity coefficient). Human RBCs bind oxygen with a $P_{50}$ of 26 mm Hg and a cooperativity coefficient of 2.6[19]. The $P_{50}$ for hHb was measured to be 12 mm Hg (Figure 3A), which is lower than that of RBCs due to absence of the allosteric effector 2,3-bisphosphoglycerate (2,3-BPG)[56]. The cooperativity coefficient of hHb was 2.6. For LtEc, the $P_{50}$ was ~29 mm Hg, with a cooperativity

coefficient of 3.3. We did not observe a significant difference in the oxygen equilibrium properties of LtEc-UP and LtEc-10D as determined by a two-sample t-test (Table 1). The comparable $P_{50}$s and similarity of the OECs for human RBCs and LtEc provides further evidence for the potential of LtEc to serve as a RBC substitute.

Oxygenated hHb and LtEc were rapidly mixed with the oxygen scavenger sodium dithionite to measure the rate of oxygen offloading. The oxygen offloading rate constant ($k_{off,O_2}$) was determined by fitting a first order rate law to the deoxygenation time course. The trailing leg from t = 0 to t = 0.05 s was due to quenching of dissolved oxygen in the buffer and was hence eliminated from the curve fit. hHb offloaded oxygen very quickly with a $k_{off,O_2}$of 39 $s^{-1}$ (Table 1), whereas human RBCs was reported to be ~5 $s^{-1}$ [55], which is much slower. This may be explained by the diffusive limitations of oxygen transport through the RBC membrane, whereas the heme in cell-free Hb is readily accessible for oxygen transport. LtEc had a $k_{off,O_2}$ of 30 $s^{-1}$, which was slower than hHb, but faster than RBCs (Figure 3B). The oxygen offloading rate is dependent on the structure of the heme pocket which regulates transport of oxygen into the surroundings. The heme pockets in the LtEc megastructure occupy the outer sections of the protein (with linkers primarily occupying the inner sections) which makes it easier for the globins to bind and offload oxygen compared to RBCs. Also, the diffusive limitations of oxygen transport through the RBC membrane contribute to the slower rate of oxygen offloading. Furthermore, the heme pockets in LtEc are smaller and more compact than those in hHb explaining the comparatively slower rate of oxygen offloading[57].

### 3.5. Auto-Oxidation Kinetics

The oxidized form of Hb (metHb) cannot bind/release oxygen and can be easily identified by the presence of a significant absorbance peak at 630 nm (Figure 3C). LtEc has a positive redox potential which reduces its conversion to metLtEc, compared to hHb which has a negative redox potential, and hence has a lower auto-oxidation rate constant[16,58,59]. The auto-oxidation rate constant of hHb was 0.033 $h^{-1}$ (which is comparable to the previously reported value of 0.043 $h^{-1}$ [12]), while that of both LtEc variants was <0.012 $h^{-1}$ (Figure 3D). This is thought to be due to the relatively smaller size of the LtEc hydrophobic heme-binding pocket as compared to hHb, thus slowing down the escape of $O_2^-$and formation of metLtEc[60]. Comparing the two LtEc variants, we observed that LtEc-UP had an auto-oxidation rate constant of 0.004 $h^{-1}$ which was almost 3 times slower than that of LtEc-10D (0.011 $h^{-1}$). It is likely that the presence of smaller MW proteins in LtEc-10D sped up oxidation and formation of metLtEc. Under physiological conditions, we desire LtEc to stay in the reduced state for as long as possible so that it can bind and release oxygen. The slower oxidation rate of LtEc-UP would enable it to stay in its reduced form for a longer period of time than LtEc-10D and much longer than hHb. Previously developed HBOCs such as Polyheme® and Oxyglobin® had auto-oxidation rate constants of 0.260 $h^{-1}$ and 0.210 $h^{-1}$ respectively, which, under physiological conditions, convert to metHb much faster than LtEc-UP[12]. This unique property of LtEc to oxidize slowly makes it a viable candidate to be used an oxygen therapeutic for a variety of applications over long time periods. Further, the slower oxidation rate of LtEc-UP compared to LtEc-E and LtEc-10D justifies the purification of an ultrapure LtEc product which is >99% in purity. One could try to achieve

higher purity (~1–10 ppm) using chromatographic techniques but it is unlikely that the biophysical properties such as oxygen equilibrium, deoxygenation kinetics, and auto-oxidation rate will improve drastically. Hence, LtEc-UP was concluded to be a suitable product that can be tested in animal models to determine its' *in vivo* performance.

### 3.6. Animal Results

Animals were randomly assigned to each experimental group (5% HSA, LtEc-10D, LtEc-UP) following a 40% exchange with 5% HSA to induce moderate anemic conditions. All animals tolerated the experiments without signs of pain or discomfort.

Both MAP and HR did not significantly differ from baseline after ET1 (Figure 4A–B). The HR for the 5% HSA control dipped to ~310 BPM after ET2 and was significantly different than the LtEc-UP group, which was maintained close to baseline along with LtEc-10D group. The total Hb (tHb), pH, $pCO_2$, and $pO_2$ followed expected trends as a result of the anemic conditions. The introduction of LtEc-UP and LtEc-10D expectedly increased the $pO_2$ and decreased the $pCO_2$. The exchange of RBCs with HSA/LtEc resulted in a drop in Hct and tHb after both ET1 and ET2. This possibly also led to an increase in the dissolved oxygen concentration in the plasma resulting in a higher than normal $pO_2$. Under these conditions it was normal for respiration to increase resulting in a drop in $pCO_2$ caused by animal hyperventilation.

The FCD, which is a marker for metabolite washout and microcirculatory pressure[61], experienced a drop that was statistically significant to baseline and ET1 after the exchange with LtEc-10D (Figure 5). Following the exchange with LtEc-UP, the FCD drop was only significant to baseline and there was no statistical significance compared to ET1 or 5% HSA. However, this drop in FCD was not entirely as a result of the toxicity of LtEc-10D or LtEc-UP, since inducing moderate anemia altered blood rheology to yield a less viscous solution. Due to the initial exchange transfusion with 5% HSA, the drop in RBC count led to a reduction in the shear stress applied to the endothelium. This resulted in reduced dilatation in the larger vessels and perfusion of fewer capillaries. Infusion of 5% HSA into the systemic circulation also increased the COP in the microcirculation, causing reabsorption of interstitial fluid into the vascular space and thus, facilitating perfusion of the capillary bed. In comparison to 5% HSA that had a COP of ~20 mm Hg, 5% LtEc-10D had a COP 4.4 mm Hg and 5% LtEc-UP had a COP of 5.6 mm Hg. Hence, after ET2 was completed with 5% HSA, the COP of the microcirculation re-equilibrated to a lower value compared to baseline. The arteriole end COP dropped from 35 mm Hg to <20 mm Hg and promoted re-absorption of interstitial fluid into the vascular space instead of promoting filtration to the surrounding tissue space. In contrast, after ET2 with LtEc-10D and LtEc-UP (both possess lower COPs than blood or 5% HSA), there was a significant drop in the COP in the microcirculation as compared to HSA infusion. In previous hemodilution studies with LtEc (ET2), dextran 70 kDa (Dex-70) was used as a hemodilutant (ET1), which had a COP of ~44 mm Hg[6,23]. Hence, after transfusion with LtEc (ET2), which had a COP of ~6–8 mm Hg, flow in arterioles was maintained due to the effectively high COP caused by the Dex-70 introduced into the circulation during ET1. Thus, the difference in choice of hemodilutant for ET1 explains the discrepancy in microcirculatory response between the previous study and this

current study. Moreover, lowering the viscosity of the blood reduces the amount of mechanotransduction experienced on the endothelial lining of the blood vessel wall[62,63]. Reduction in mechanotransduction lowers the concentration of endothelial NO synthase (eNOS) that is expressed by endothelial cells and as a result lowers the concentration of NO, a potent vasodilator[64–66]. As a result of lower NO concentration, the internal microvascular pressure falls resulting in the collapse of a number of capillaries and a drop in FCD. Following the exchange of LtEc-UP versus LtEc-10D there was a statistically significant drop in FCD for LtEc-10D but not for LtEc-UP compared to ET1. Since all other properties of the LtEc variants were identical, it was possible that the higher amount of impurities in LtEc-10D compared to LtEc-UP compromised microvascular flow and thus causing a significant drop in FCD. This provided further evidence for the necessity to purify LtEc-UP to the reported purity and that this 99% pure product was sufficient to maintain systemic parameters and FCD *in vivo*.

LtEc is known to possess additional biophysical properties, such as increased molecular diameter, that are crucial for the development of an effective HBOC[67,68]. This explains the lack of vasoactivity, since the large molecular diameter of LtEc prevents tissue extravasation and reduces the effect of NO scavenging and subsequent vasoconstriction that was observed with other HBOCs. Both LtEc products maintained arteriolar and venular diameter compared to baseline (Figure 6A and C), but induced a decrease in hemodynamic flow in the microcirculation, which was statistically significant in the venules (Figure 6D) but not in the arterioles (Figure 6B). However, the impaired flow could be a result of the low concentration of the HBOC that was used. The initial tHb concentration for the animals was ~15 g/dL with both LtEc-10D and LtEc-UP having a concentration of 5 g/dL, which was not enough to compensate for the loss of tHb resulting from the exchange transfusion thus resulting in less than optimal flow. However, there was a difference in flow in the arterioles when comparing LtEc-UP and LtEc-10D after inducing anemic conditions in the animals (Figure 6B) but was not statistically different. With the concentration of impurities present in LtEc-10D being much higher than in LtEc-UP, it was possible that these impurities disrupted blood flow by promoting greater RBC aggregation and thus reducing flow. The fluid velocity in the arterioles is naturally faster than those of their venule counterparts, which is why arteriole flow is more sensitive to flow disruption than venular flow. The venular flow did change when comparing the two LtEc products, but saw a significant drop as compared to the HSA control (Figure 6D). Compared to the LtEc solutions, the 5% HSA solution perfused blood vessels with greater success due to its higher COP. Our results suggest that a 99% pure LtEc product was sufficient to promote better microcirculatory outcomes (i.e. sustaining a higher FCD), which is a promising result and supports future development of LtEc as a RBC substitute.

## 4. Conclusion

We devised a strategy to purify ultra-pure LtEc using TFF. Quantitative assessment using SEC-HPLC concluded that the purity attained was >99% with effective removal of unwanted protein impurities. LtEc-UP had a slower rate of auto-oxidation than LtEc-10D while maintaining oxygen equilibrium curves similar to human RBCs and oxygen offloading kinetics similar to acellular Hb. These advantages of LtEc-UP open up avenues for its use as

an oxygen therapeutic for a wide range of applications apart from its use in transfusion medicine, such as a cold static organ preservation solution and as a cell culture media supplement. Administration into animals showed that LtEc-UP maintained MAP, HR, and blood gases while having a significantly lower reduction in FCD than LtEc-10D. Furthermore, flow in arterioles did not return back to baseline but did not differ significantly compared to the control of 5% HSA. These animal results combined with the *in vitro* biophysical characterization results show that LtEc-UP has promise as an oxygen therapeutic.

## Acknowledgements

We thank Dr James Lee (The Ohio State University) for allowing us to use his dynamic light scattering (DLS) instrument and Dr. David Wood (The Ohio State University) for allowing us to use his ultracentrifuge. This work was supported by National Institutes of Health grant NHLBI R01HL138116.

## References

(1). Taveau JC; Boisset N; Vinogradov SN; Lamy JN Three-Dimensional Reconstruction of Lumbricus Terrestris Hemoglobin at 22 Å Resolution: Intramolecular Localization of the Globin and Linker Chains. J. Mol. Biol 1999, 289 (5), 1343–1359. 10.1006/jmbi.1999.2824. [PubMed: 10373371]

(2). Strand K; Knapp JE; Bhyravbhatla B; Royer WE Crystal Structure of the Hemoglobin Dodecamer from Lumbricus Erythrocruorin: Allosteric Core of Giant Annelid Respiratory Complexes. J. Mol. Biol 2004, 344 (1), 119–134. 10.1016/j.jmb.2004.08.094. [PubMed: 15504406]

(3). Zhu H; Ownby DW; Riggs CK; Nolasco NJ; Stoops JK; Riggs AF Assembly of the Gigantic Hemoglobin of the Earthworm Lumbricus Terrestris. J. Biol. Chem 1996, 271 (47), 30007–30021. 10.1074/jbc.271.47.30007. [PubMed: 8939947]

(4). Palmer AF; Intaglietta M Blood Substitutes. Annu. Rev. Biomed. Eng 2014, 16 (1), 77–101. 10.1146/annurev-bioeng-071813-104950. [PubMed: 24819476]

(5). Le Gall T; Polard V; Rousselot M; Lotte A; Raouane M; Lehn P; Opolon P; Leize E; Deutsch E; Zal F; Montier T In Vivo Biodistribution and Oxygenation Potential of a New Generation of Oxygen Carrier. J. Biotechnol 2014, 187, 1–9. 10.1016/j.jbiotec.2014.07.008. [PubMed: 25034433]

(6). Elmer J; Zorc K; Rameez S; Zhou Y; Cabrales P; Palmer AF Hypervolemic Infusion of Lumbricus Terrestris Erythrocruorin Purified by Tangential-Flow Filtration. Transfusion 2012, 52 (8), 1729–1740. 10.1111/j.1537-2995.2011.03523.x. [PubMed: 22304397]

(7). Walder RY; Andracki ME; Walder JA Preparation of Intramolecularly Cross-Linked Hemoglobins. Methods Enzymol. 1994, 231 (C), 274–280. 10.1016/0076-6879(94)31019-X. [PubMed: 8041257]

(8). Winslow RM MP4, a New Nonvasoactive Polyethylene Glycol-Hemoglobin Conjugate. Artif. Organs 2004, 28 (9), 800–806. 10.1111/j.1525-1594.2004.07392.x. [PubMed: 15320943]

(9). Manjula BN; Tsai A; Upadhya R; Perumalsamy K; Smith PK; Malavalli A; Vandegriff K; Winslow RM; Intaglietta M; Prabhakaran M; Friedman JM; Acharya AS Site-Specific PEGylation of Hemoglobin at Cys-93(β): Correlation between the Colligative Properties of the PEGylated Protein and the Length of the Conjugated PEG Chain. Bioconjug. Chem 2003, 14 (2), 464–472. 10.1021/bc0200733. [PubMed: 12643758]

(10). Manjula BN; Tsai AG; Intaglietta M; Tsai C-HH; Ho C; Smith PK; Perumalsamy K; Kanika ND; Friedman JM; Acharya SA Conjugation of Multiple Copies of Polyethylene Glycol to Hemoglobin Facilitated through Thiolation: Influence on Hemoglobin Structure and Function. Protein J. 2005, 24 (3), 133–146. 10.1007/s10930-005-7837-2. [PubMed: 16096719]

(11). Acharya SA; Friedman JM; Manjula BN; Intaglietta M; Tsai AG; Winslow RM; Malavalli A; Vandegriff K; Smith PK Enhanced Molecular Volume of Conservatively Pegylated Hb: (SP-PEG5K)6-HbA Is Non-Hypertensive. Artif. Cells. Blood Substit. Immobil. Biotechnol 2005, 33 (3), 239–255. 10.1081/bio-200066365. [PubMed: 16152690]

(12). Meng F; Kassa T; Jana S; Wood F; Zhang X; Jia Y; D'Agnillo F; Alayash AI Comprehensive Biochemical and Biophysical Characterization of Hemoglobin-Based Oxygen Carrier Therapeutics: All HBOCs Are Not Created Equally. Bioconjug. Chem 2018, 29 (5), 1560–1575. 10.1021/acs.bioconjchem.8b00093. [PubMed: 29570272]

(13). Sakai H; Sou K; Horinouchi H; Kobayashi K; Tsuchida E Review of Hemoglobin-Vesicles as Artificial Oxygen Carriers. Artif. Organs 2009, 33 (2), 139–145. 10.1111/j.1525-1594.2008.00698.x. [PubMed: 19178458]

(14). Bäumler H; Xiong Y; Liu ZZ; Patzak A; Georgieva R Novel Hemoglobin Particles-Promising New-Generation Hemoglobin-Based Oxygen Carriers. Artif. Organs 2014, 38 (8), 708–714. 10.1111/aor.12331. [PubMed: 24962099]

(15). Xiong Y; Liu ZZ; Georgieva R; Smuda K; Steffen A; Sendeski M; Voigt A; Patzak A; Bäumler H Nonvasoconstrictive Hemoglobin Particles as Oxygen Carriers. ACS Nano 2013, 7 (9), 7454–7461. 10.1021/nn402073n. [PubMed: 23915101]

(16). Elmer J; Palmer AF Biophysical Properties of Lumbricus Terrestris Erythrocruorin and Its Potential Use as a Red Blood Cell Substitute. J. Funct. Biomater 2012, 3 (4), 49–60. 10.3390/jfb3010049. [PubMed: 24956515]

(17). Rousselot M; Delpy E; Drieu La Rochelle C; Lagente V; Pirow R; Rees J-F; Hagege A; Le Guen D; Hourdez S; Zal F Arenicola Marina Extracellular Hemoglobin: A New Promising Blood Substitute. Biotechnol. J 2006, 1 (3), 333–345. 10.1002/biot.200500049. [PubMed: 16897713]

(18). Le Pape F; Cosnuau-Kemmat L; Richard G; Dubrana F; Férec C; Zal F; Leize E; Delépine P HEMOXCell, a New Oxygen Carrier Usable as an Additive for Mesenchymal Stem Cell Culture in Platelet Lysate-Supplemented Media. Artif. Organs 2017, 41 (4), 359–371. 10.1111/aor.12892. [PubMed: 28326561]

(19). Oneglia C; Fabris C; Modica A; Rossi CM; Bigo P; Ricco G The Oxygen Affinity of Normal Human Whole Blood Measured by Double Tonometry. I. P50 and n Factor. Boll. Soc. Ital. Biol. Sper 1984, 60 (2), 421–427. [PubMed: 6712804]

(20). Libardi SH; Alves FR; Tabak M Interaction of Glossoscolex Paulistus Extracellular Hemoglobin with Hydrogen Peroxide: Formation and Decay of Ferryl-HbGp. Int. J. Biol. Macromol 2018, 111, 271–280. 10.1016/j.ijbiomac.2017.12.147. [PubMed: 29305213]

(21). Bachega JFR; Maluf FV; Andi B; Pereira HDM; Carazzollea MF; Orville AM; Tabak M; Brandão-Neto J; Garratt RC; Reboredo EH The Structure of the Giant Haemoglobin from Glossoscolex Paulistus. Acta Crystallogr. Sect. D Biol. Crystallogr 2015, 71, 1257–1271. 10.1107/S1399004715005453. [PubMed: 26057666]

(22). Carvalho FAO; Alves FR; Carvalho JWP; Tabak M Guanidine Hydrochloride and Urea Effects upon Thermal Stability of Glossoscolex Paulistus Hemoglobin (HbGp). Int. J. Biol. Macromol 2015, 74, 18–28. 10.1016/j.ijbiomac.2014.11.012. [PubMed: 25433131]

(23). Elmer J; Palmer A; Cabrales P Oxygen Delivery during Extreme Anemia with Ultra-Pure Earthworm Hemoglobin. NIH Public Access 2013, 91 (858), 852–859. 10.1016/j.lfs.2012.08.036.Oxygen.

(24). A. G. Tsai; Intaglietta M; Sakai H; Delpy E; Drieu La Rochelle C; Rousselot M; Zal F Microcirculation and NO-CO Studies of a Natural Extracellular Hemoglobin Developed for an Oxygen Therapeutic Carrier. Curr. Drug Discov. Technol 2012, 9 (3), 166–172. 10.2174/157016312802650814. [PubMed: 22564165]

(25). Rousselot M; Delpy E; La Rochelle CD; Lagente V; Pirow R; Rees JF; Hagege A; Le Guen D; Hourdez S; Zal F Arenicola Marina Extracellular Hemoglobin: A New Promising Blood Substitute. Biotechnol. J 2006, 1 (3), 333–345. 10.1002/biot.200500049. [PubMed: 16897713]

(26). Le Pape F; Bossard M; Dutheil D; Rousselot M; Polard V; Férec C; Leize E; Delépine P; Zal F Advancement in Recombinant Protein Production Using a Marine Oxygen Carrier to Enhance Oxygen Transfer in a CHO-S Cell Line. Artif. Cells, Nanomedicine, Biotechnol 2015, 43 (3), 186–195. 10.3109/21691401.2015.1029632.

(27). Rodriguez-Brotons A; Bietiger W; Peronet C; Langlois A; Magisson J; Mura C; Sookhareea C; Polard V; Jeandidier N; Zal F; Pinget M; Sigrist S; Maillard E Comparison of Perfluorodecalin and HEMOXCell as Oxygen Carriers for Islet Oxygenation in an In Vitro Model of Encapsulation. Tissue Eng. Part A 2016, 22 (23–24), 1327–1336. 10.1089/ten.tea.2016.0064. [PubMed: 27796164]

(28). Teh ES; Zal F; Polard V; Menasché P; Chambers DJ HEMO2life as a Protective Additive to Celsior Solution for Static Storage of Donor Hearts Prior to Transplantation. Artif. Cells, Nanomedicine Biotechnol 2017, 45 (4), 717–722. 10.1080/21691401.2016.1265974.

(29). Glorion M; Polard V; Favereau F; Hauet T; Zal F; Fadel E; Sage E Prevention of Ischemia-Reperfusion Lung Injury during Static Cold Preservation by Supplementation of Standard Preservation Solution with HEMO2life® in Pig Lung Transplantation Model. Artif. Cells, Nanomedicine Biotechnol 2018, 46 (8), 1773–1780. 10.1080/21691401.2017.1392315.

(30). Thuillier R; Delpy E; Matillon X; Kaminski J; Kasil A; Soussi D; Danion J; Sauvageon Y; Rod X; Donatini G; Barrou B; Badet L; Zal F; Hauet T Preventing Acute Kidney Injury during Transplantation: The Application of Novel Oxygen Carriers. Expert Opin. Investig. Drugs 2019, 28 (7), 643–657. 10.1080/13543784.2019.1628217.

(31). Chen W-T; Chen Y-C; Liou H-H; Chao C-Y Structural Basis for Cooperative Oxygen Binding and Bracelet-Assisted Assembly of Lumbricus Terrestris Hemoglobin. Sci. Rep 2015, 5 (1), 9494 10.1038/srep09494. [PubMed: 25897633]

(32). Zimmerman D; Dienes J; Abdulmalik O; Elmer JJ Purification of Diverse Hemoglobins by Metal Salt Precipitation. Protein Expr. Purif 2016, 125, 74–82. 10.1016/j.pep.2015.09.006. [PubMed: 26363116]

(33). Elmer J; Palmer AF; Cabrales P Oxygen Delivery during Extreme Anemia with Ultra-Pure Earthworm Hemoglobin. Life Sci. 2012, 91 (17–18), 852–859. 10.1016/j.lfs.2012.08.036. [PubMed: 22982347]

(34). Valembois P; Roch P; Lassegues M Evidence of Plasma Clotting System in Earthworms. J. Invertebr. Pathol 1988, 51 (3), 221–228. 10.1016/0022-2011(88)90029-8.

(35). Timm B; Abdulmalik O; Chakrabarti A; Elmer J Purification of Lumbricus Terrestris Erythrocruorin (LtEc) with Anion Exchange Chromatography. J. Chromatogr. B 2020, 122162 10.1016/j.jchromb.2020.122162.

(36). Palmer AF; Sun G; Harris DR Tangential Flow Filtration of Hemoglobin. Biotechnol. Prog 2009, 25 (1), 189–199. 10.1002/btpr.119. [PubMed: 19224583]

(37). Drabkin DL; Austin JH Spectrophotometric Studies Ii. Preparations From Washed Blood Cells; Nitric Oxide Hemoglobin and Sulfhemoglobin. J. Biol. Chem 1935, 112 (1), 51–65.

(38). Winterbourn CC Oxidative Reactions of Hemoglobin. Methods Enzymol. 1990, 186 (C), 265–272. 10.1016/0076-6879(90)86118-F. [PubMed: 2172706]

(39). Fanelli MRR; Chiancone E; Vecchini P; Antonini E; Rossi Fanelli MR; Antonini E Studies on Erythrocruorin. J. Mol. Biol 1972, 141 (1), 278–283. 10.1016/0022-2836(72)90164-7.

(40). Fanelli MRR; Chiancone E; Vecchini P; Antonini E Studies on Erythrocruorin. I. Physicochemical Properties of Earthworm Erythrocruorin. Arch. Biochem. Biophys 1970, 141 (1), 278–283. 10.1016/0003-9861(70)90133-5. [PubMed: 5480115]

(41). Schneider CA; Rasband WS; Eliceiri KW NIH Image to ImageJ: 25 Years of Image Analysis. Nature Methods. 7 2012, pp 671–675. 10.1038/nmeth.2089. [PubMed: 22930834]

(42). HILL A The Possible Effects of the Aggregation of the Molecules of Haemoglobin on Its Dissociation Curves. J Physiol (Lond). 1 1, 1910, pp 4–7.

(43). Rameez S; Banerjee U; Fontes J; Roth A; Palmer AF Reactivity of Polymersome Encapsulated Hemoglobin with Physiologically Important Gaseous Ligands: Oxygen, Carbon Monoxide, and Nitric Oxide. Macromolecules 2012, 45 (5), 2385–2389. 10.1021/ma202739f. [PubMed: 22865934]

(44). Rameez S; Palmer AF Simple Method for Preparing Poly(Ethylene Glycol)-Surface-Conjugated Liposome-Encapsulated Hemoglobins: Physicochemical Properties, Long-Term Storage Stability, and Their Reactions with O2, CO, and NO. Langmuir 2011, 27 (14), 8829–8840. 10.1021/la201246m. [PubMed: 21678920]

(45). Endrich B; Asaishi K; Götz A; Meßmer K Technical Report—a New Chamber Technique for Microvascular Studies in Unanesthetized Hamsters. Res. Exp. Med 1980, 177 (2), 125–134. 10.1007/BF01851841.

(46). Intaglietta M; Silverman NR; Tompkins WR Capillary Flow Velocity Measurements in Vivo and in Situ by Television Methods. Microvasc. Res 1975, 10 (2), 165–179. 10.1016/0026-2862(75)90004-7. [PubMed: 1186524]

(47). Lipowsky HH; Zweifach BW Application of the “Two-Slit” Photometric Technique to the Measurement of Microvascular Volumetric Flow Rates. Microvasc. Res 1978, 15 (1), 93–101. 10.1016/0026-2862(78)90009-2. [PubMed: 634160]

(48). Intaglietta M; Tompkins WR Microvascular Measurements by Video Image Shearing and Splitting. Microvasc. Res 1973, 5 (3), 309–312. 10.1016/0026-2862(73)90042-3. [PubMed: 4709728]

(49). Muzzelo C; Neely C; Shah P; Abdulmalik O; Elmer J Prolonging the Shelf Life of Lumbricus Terrestris Erythrocruorin for Use as a Novel Blood Substitute. Artif. Cells, Nanomedicine, Biotechnol 2018, 46 (1), 39–46. 10.1080/21691401.2017.1290645.

(50). Daniel E; Lustig A; David MM; Tsfadia Y Towards a Resolution of the Long-Standing Controversy Regarding the Molecular Mass of Extracellular Erythrocruorin of the Earthworm Lumbricus Terrestris. Biochim. Biophys. Acta - Proteins Proteomics 2003, 1649 (1), 1–5. 10.1016/S1570-9639(03)00023-2.

(51). Zhu H; Hargrove M; Xie Q; Nozaki Y; Linse K; Smith SS; Olson JS; Riggs AF Stoichiometry of Subunits and Heme Content of Hemoglobin from the Earthworm Lumbricus Terrestris. J. Biol. Chem 1996, 271 (47), 29999–30006. 10.1074/jbc.271.47.29999. [PubMed: 8939946]

(52). Spivack K; Tucker M; Zimmerman D; Nicholas M; Abdulmalik O; Comolli N; Elmer J Increasing the Stability of Lumbricus Terrestris Erythrocruorin via Poly(Acrylic Acid) Conjugation. Artif. Cells, Nanomedicine, Biotechnol 2018, 46 (sup2), 1137–1144. 10.1080/21691401.2018.1480491.

(53). Rajesh A; Zimmerman D; Spivack K; Abdulmalik O; Elmer J Glutaraldehyde Cross-Linking Increases the Stability of Lumbricus Terrestris Erythrocruorin. Biotechnol. Prog 2018, 34 (2), 521–528. 10.1002/btpr.2593. [PubMed: 29226612]

(54). Stetefeld J; McKenna SA; Patel TR Dynamic Light Scattering: A Practical Guide and Applications in Biomedical Sciences. Biophys. Rev 2016, 8 (4), 409–427. 10.1007/s12551-016-0218-6. [PubMed: 28510011]

(55). Coin JT; Olson JS The Rate of Oxygen Uptake by Human Red Blood Cells. J. Biol. Chem 1979, 254 (4), 1178–1190. [PubMed: 762123]

(56). Bunn HF; Briehl RW The Interaction of 2,3-Diphosphoglycerate with Various Human Hemoglobins. J. Clin. Invest 1970, 49 (6), 1088–1095. 10.1172/JCI106324. [PubMed: 5422014]

(57). Royer WE; Sharma H; Strand K; Knapp JE; Bhyravbhatla B Lumbricus Erythrocruorin at 3.5 Å Resolution: Architecture of a Megadalton Respiratory Complex. Structure 2006, 14 (7), 1167–1177. 10.1016/j.str.2006.05.011. [PubMed: 16843898]

(58). Harrington JP; Kobayashi S; Dorman SC; Zito SL; Hirsch RE Acellular Invertebrate Hemoglobins as Model Therapeutic Oxygen Carriers: Unique Redox Potentials. Artif. Cells, Blood Substitutes, Biotechnol 2007, 35 (1), 53–67. 10.1080/10731190600974491.

(59). Dorman SC; Harrington JP; Martin MS; Johnson TV Determination of the Formal Reduction Potential of Lumbricus Terrestris Hemoglobin Using Thin Layer Spectroelectrochemistry. J. Inorg. Biochem 2004, 98 (1), 185–188. 10.1016/j.jinorgbio.2003.10.004. [PubMed: 14659648]

(60). Gow AJ; Payson AP; Bonaventura J Invertebrate Hemoglobins and Nitric Oxide: How Heme Pocket Structure Controls Reactivity. J. Inorg. Biochem 2005, 99 (4), 903–911. 10.1016/j.jinorgbio.2004.12.001. [PubMed: 15811507]

(61). Cabrales P; Tsai AG; Intaglietta M Microvascular Pressure and Functional Capillary Density in Extreme Hemodilution with Low-and High-Viscosity Dextran and a Low-Viscosity Hb-Based O 2 Carrier. Am. J. Physiol. Circ. Physiol 2004, 287 (1), H363–H373. 10.1152/ajpheart.01039.2003.

(62). Cabrales P; Tsai AG; Intaglietta M Increased Plasma Viscosity Prolongs Microhemodynamic Conditions during Small Volume Resuscitation from Hemorrhagic Shock. Resuscitation 2008, 77 (3), 379–386. 10.1016/j.resuscitation.2008.01.008. [PubMed: 18308459]

(63). Cabrales P; Intaglietta M; Tsai AG Transfusion Restores Blood Viscosity and Reinstates Microvascular Conditions from Hemorrhagic Shock Independent of Oxygen Carrying Capacity. Resuscitation 2007, 75 (1), 124–134. 10.1016/j.resuscitation.2007.03.010. [PubMed: 17481796]

(64). Fukumura D; Jain RK Role of Nitric Oxide in Angiogenesis and Microcirculation in Tumors. Cancer Metastasis Rev. 1998, 17 (1), 77–89. 10.1023/A:1005908805527. [PubMed: 9544424]

(65). Lundberg JO; Weitzberg E; Gladwin MT The Nitrate–Nitrite–Nitric Oxide Pathway in Physiology and Therapeutics. Nat. Rev. Drug Discov 2008, 7 (2), 156–167. 10.1038/nrd2466. [PubMed: 18167491]

(66). Liu S; Premont RT; Kontos CD; Huang J; Rockey DC Endothelin-1 Activates Endothelial Cell Nitric-Oxide Synthase via Heterotrimeric G-Protein Bγ Subunit Signaling to Protein Kinase B/Akt. J. Biol. Chem 2003, 278 (50), 49929–49935. 10.1074/jbc.M306930200. [PubMed: 14523027]

(67). Cabrales P; Intaglietta M Blood Substitutes. ASAIO J. 2013, 59 (4), 337–354. 10.1097/MAT.0b013e318291fbaa. [PubMed: 23820271]

(68). Fushitani K; Imai K; Riggs AF Oxygenation Properties of Hemoglobin from the Earthworm, Lumbricus Terrestris. Effects of PH, Salts, and Temperature. J. Biol. Chem 1986, 261 (18), 8414–8423. [PubMed: 3722158]

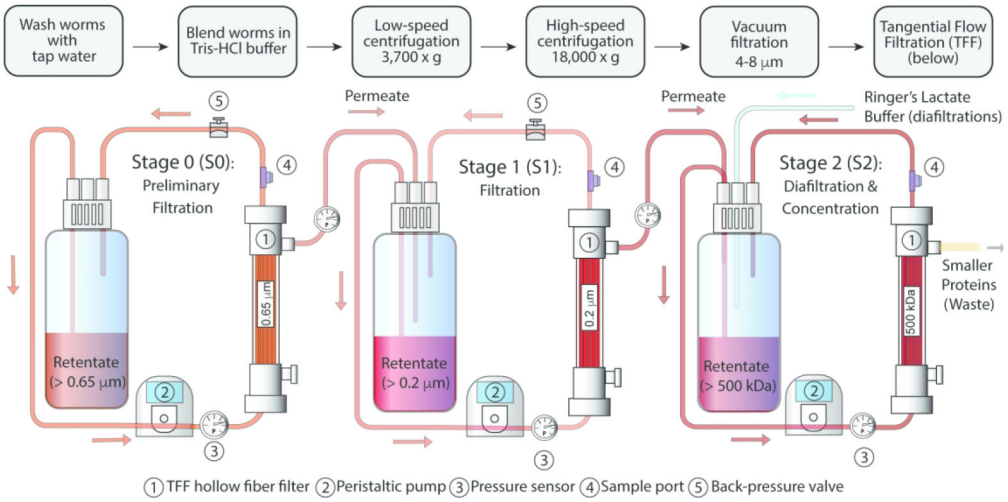


**Figure 1:**

Schematic of LtEc purification process with multi-stage tangential flow filtration (TFF). Filtration in stages 0 and 1 eliminated larger components and bacterial contaminants from the product. Diafiltration on the stage 2 filter eliminated smaller proteins. The product was concentrated in stage 2 and stored for future use.

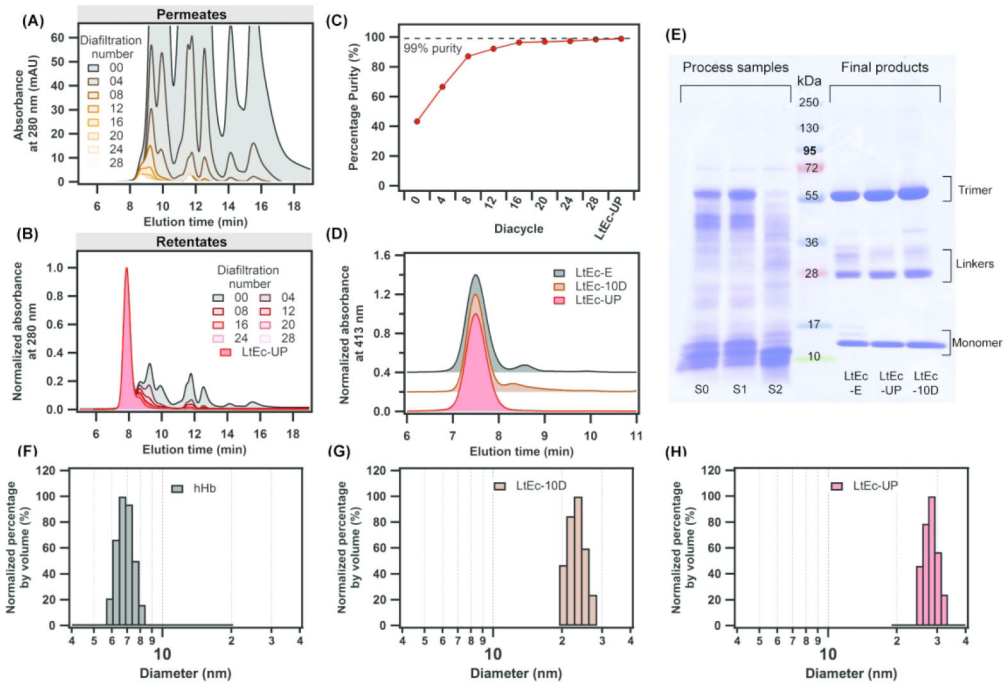


**Figure 2:**

Purity and size assessment of LtEc products. **(A)** Permeate and **(B)** Retentate SEC-HPLC chromatograms of the 500 kDa permeate/retentate monitored at 280 nm. The sharp peak at ~7.81 mins corresponds to the target protein LtEc, and the remaining peaks correspond to smaller MW proteins. A reduction in the presence of smaller MW proteins in the retentate was observed with increasing number of diacycles. **(C)** Percentage purity of LtEc in the retentate increased from ~43% to >99% after 30 diacycles. **(D)** SEC-HPLC chromatogram monitored at a wavelength of 413 nm for LtEc-E (a product previously purified in our lab[6]), LtEc-10D (a product recently replicated with the same processing conditions used to produce LtEc-E), and LtEc-UP (a product purified using the improved methods as described in this work). The trailing leg of impurities was eliminated in LtEc-UP compared to LtEc-E and LtEc-10D. **(E)** SDS-PAGE analysis throughout the TFF purification process. Lanes 1–3 denote process samples (S0 = Stage 0 retentate; S1 = Stage 1 retentate; S2 = Stage 2 retentate before diafiltration, see Figure 1). Lane 4 is the protein MW ladder, and lanes 5–7 denote variants of purified LtEc as previously described. Fewer impurities were observed in Lane 6 as compared to the other lanes. DLS size analysis of hHb and LtEc variants showed that LtEc-UP **(H)** had a diameter of ~28 nm as compared to 24 nm for LtEc-10D **(G)** and 6.5 nm for hHb **(F)**.

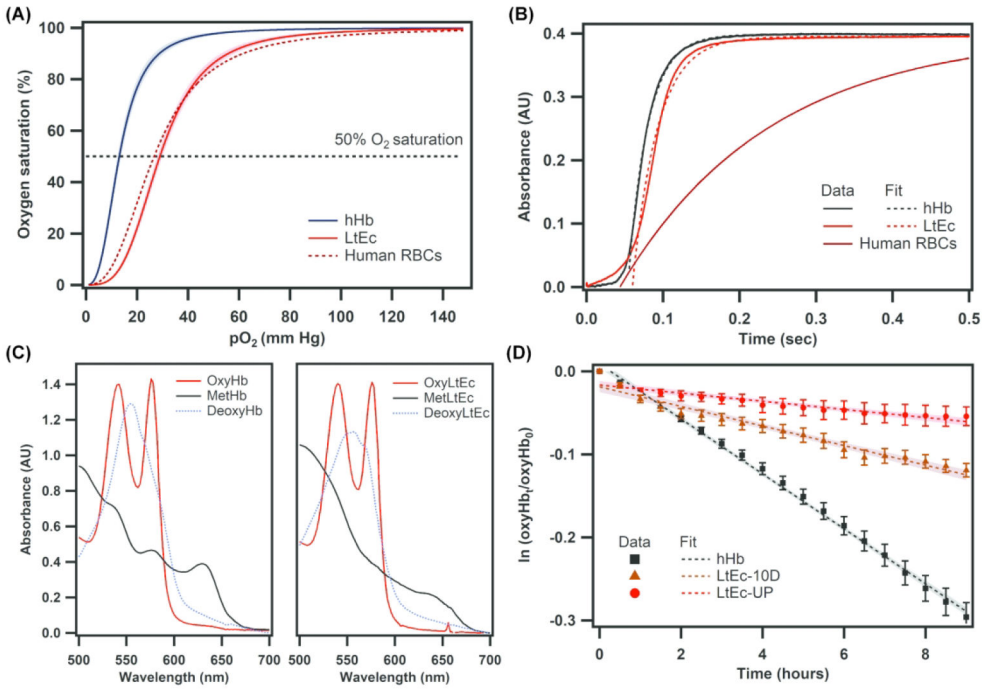


**Figure 3.**

Oxygen binding characteristics of LtEc. **(A)** Oxygen equilibrium curves (OEC) denoting the similarity between the oxygen binding properties of LtEc and human RBCs[19]. Shaded regions denote the 95% confidence interval of curve fits. **(B)** Stopped-flow deoxygenation kinetics of hHb and LtEc compared to human RBCs[55]. LtEc shows oxygen offloading behavior similar to hHb rather than human RBCs. **(C)** UV-visible spectra of oxy, deoxy, and metHb species of hHb and LtEc. **(D)** Auto-oxidation rate comparison indicating that LtEc-UP oxidizes slower than LtEc-10D and hHb. The natural log of oxygenated species at the measurement time point was divided by the oxygenated species at the initial time point and is plotted on the y-axis. Vertical bars denote the standard deviation of 3 measurements. Shaded regions denote the 95% confidence interval of curve fits.

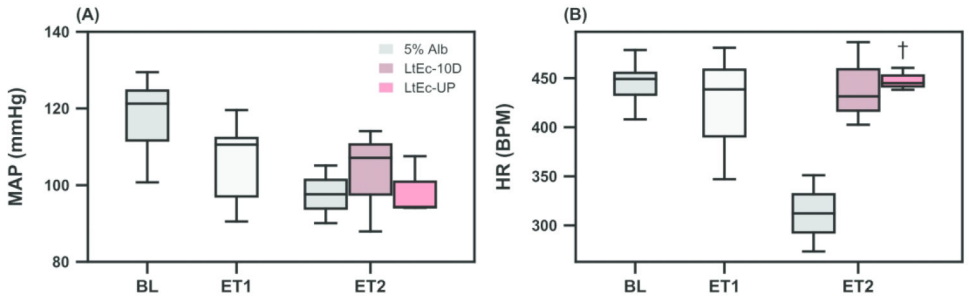


**Figure 4: Systematic parameters.**

**(A)** Mean arterial pressure (MAP) measured in mmHg at baseline (BL), after exchange transfusion 1 (ET1), and after exchange transfusion 2 (ET2). **(B)** Heart rate (HR) measured in beats per minute (bpm) at BL, ET1 and ET2. *, compared to Baseline and †, compared to 5% HSA ($p<0.05$).

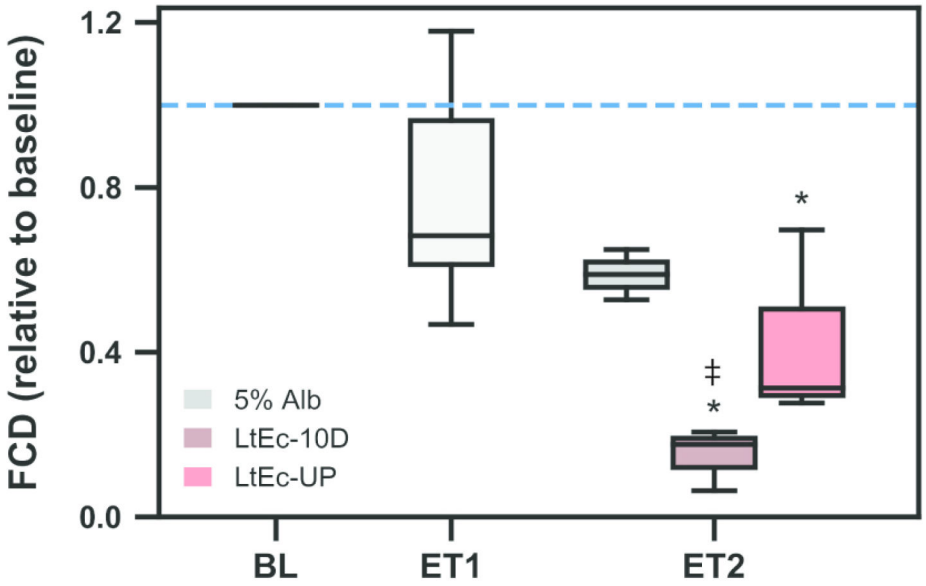


**Figure 5:**
Functional capillary density relative to baseline, * $p < 0.05$ compared to Baseline and ‡ $p < 0.05$ compared to ET1.

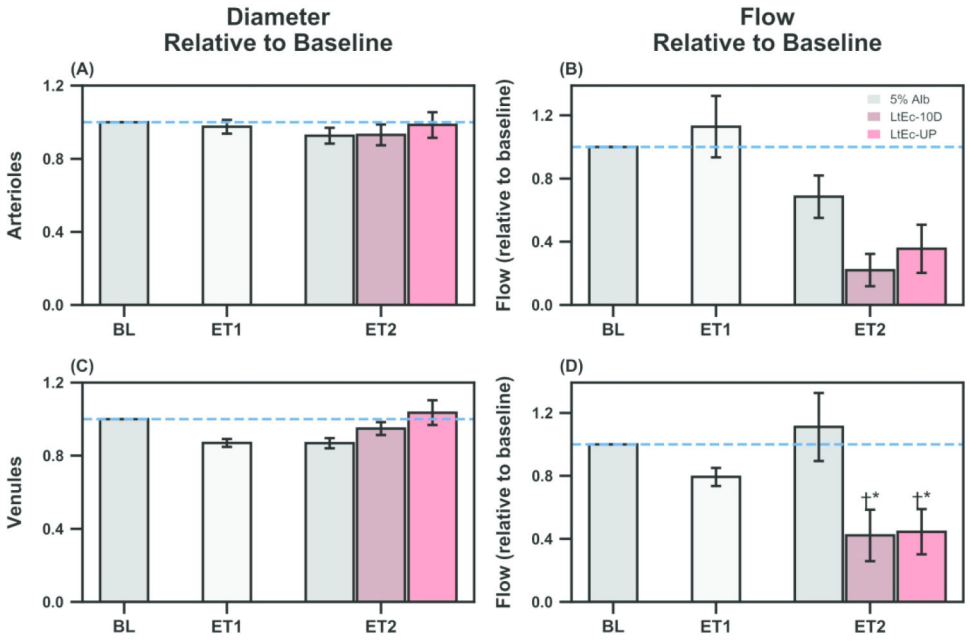


**Figure 6: Diameter and flow for arterioles and venules –**

**(A)** Diameter effects of all sized arterioles (20–100 μm), **(B)** flow effects of all sized arterioles (20–100 μm), **(C)** diameter effects of all sized venules (30–80 μm) **(D)** flow effects of all sized venules (30–80 μm) - relative to baseline during the initial phase (BL), following the initial exchange transfusion of HSA **(ET1)** and following exchange transfusion of HSA or LtEc-10D or LtEc-UP **(ET2)**. *, compared to BL and †, compared to 5% HSA group ($P<0.05$).

**Table1:**

Biophysical properties of hHb, LtEc-UP and LtEc-10D.

| | hHb | LtEc-UP | LtEc-10D |
|---|---|---|---|
| Concentration (g/dL) | 22.3 ± 1.67 | 5.14 ± 0.42 | 4.97 ± 1.06 |
| MetHb (%) | 2.70 ± 1.17 | 2.38 ± 1.27 | 2.02 ± 0.96 |
| Diameter (nm) | 6.51 ± 0.61 | 28.67 ± 2.93 * | 24.07 ± 3.07 |
| $P_{50}$ (mm Hg) | 13.07 ± 2.80 | 28.97 ± 2.84 * | 27.37 ± 2.32 * |
| Cooperativity (n) | 2.60 ± 0.15 | 3.24 ± 0.39 * | 3.46 ± 0.11 * |
| $k_{ox}$ ($h^{-1}$) | 0.033 ± 0.012 | 0.004 ± 0.001 *≠ | 0.011 ± 0.004 * |
| $k_{off,o2}$ ($s^{-1}$) | 38.91 ± 0.03 | 30.65 ± 0.07 | 29.82 ± 0.04 * |
| Viscosity (cP) at 316 $s^{-1}$ | - | 3.2 ± 0.2 | 2.0 ± 0.3 |
| COP (mm Hg) | - | 5.6 ± 2.0 | 4.4 ± 2.0 |

* $p<0.05$ compared to hHb,

≠ $p<0.05$ compared to LtEc-10D

**Table 2:**

Total Hb, Hct and blood gases for HSA, LtEc-10D and LtEc-UP treated animals.

| | | | | | |
|---|---|---|---|---|---|
| **HSA (n=3)** | | | | | |
| | **tHb (g/dL)** | **Hct (%)** | **pH** | **$pCO_2$ (mm Hg)** | **$pO_2$ (mm Hg)** |
| Baseline | 15.7 ± 0.2 | 51 ± 2 | 7.355 ± 0.016 | 53.8 ± 2.4 | 59.2 ± 4.8 |
| ET1 | 9.8 ± 0.5 | 32 ± 1 | 7.343 ± 0.033 | 53.5 ± 2.9 | 58.4 ± 7.3 |
| ET2 | 8.1 ± 0.4 | 24 ± 1 | 7.357 ± 0.039 | 48.6 ± 1.1 | 65.2 ± 0.2 |
| **LtEc-10D (n=3)** | | | | | |
| | **tHb (g/dL)** | **Hct (%)** | **pH** | **$pCO_2$ (mm Hg)** | **$pO_2$ (mm Hg)** |
| Baseline | 15.0 ± 0.4 | 48 ± 2 | 7.360 ± 0.009 | 57.3 ± 1.4 | 66.4 ± 2.1 |
| ET1 | 9.7 ±0.6 | 30 ± 3 | 7.353 ± 0.013 | 50.2 ± 1.6 | 74.6 ± 3.6 |
| ET2 | 7.5 ±0.5 | 23 ± 1 | 7.403 ± 0.040 | 35.5 ± 4.1 | 108.4 ± 12.4 |
| **LtEc-UP (n=3)** | | | | | |
| | **tHb (g/dL)** | **Hct (%)** | **pH** | **$pCO_2$ (mm Hg)** | **$pO_2$ (mm Hg)** |
| Baseline | 14.7 ± 0.5 | 47 ± 2 | 7.350 ± 0.024 | 55.4 ± 1.7 | 64.8 ± 4.8 |
| ET1 | 9.7 ± 0.3 | 32 ± 1 | 7.336 ± 0.029 | 50.4 ± 4.1 | 76.2 ± 4.3 |
| ET2 | 7.9 ± 0.1 | 23 ± 1 | 7.416 ± 0.009 | 34.3 ± 1.5 | 104.7 ± 3.4 |